NIH Public Access
Author Manuscript
Dalton Trans. Author manuscript; available in PMC 2012 May 01.

Published in final edited form as:
Dalton Trans. 2011 April 28; 40(16): 4147–4154. doi:10.1039/c1dt00001b.

Solution studies of dinuclear polyamine-linked platinum-based antitumour complexes†

Rasha A. Ruhayel[a,c], **Ibrahim Zgani**[b], **Susan J. Berners-Price**[*,a,c], and **Nicholas P. Farrell**[*,b,c]

[a]School of Biomedical, Biomolecular & Chemical Sciences, The University of Western Australia, 35 Stirling Highway, Crawley, WA, 6009, Australia

[b]Department of Chemistry, Virginia Commonwealth University, Richmond, Virginia, 23284-2006, USA

[c]Institute for Glycomics, Gold Coast Campus, Griffith University, Queensland, 4222, Australia

Abstract

The aquation profiles of two novel dinuclear polyamine-linked, platinum-based antitumour complexes [{*trans*-PtCl($^{15}NH_3$)$_2$}$_2${μ-($^{15}NH_2$(CH$_2$)$_6$$^{15}NH_2$(CH$_2$)$_6$$^{15}NH_2$)}]$^{3+}$ (BBR3007, 1,1/*t,t*-6,6, **1**) and [{*trans*-PtCl($^{15}NH_3$)$_2$}$_2${μ-($^{15}NH_2$(CH$_2$)$_6$$^{15}NH_2$(CH$_2$)$_2$$^{15}NH_2$(CH$_2$)$_6$$^{15}NH_2$)}]$^{4+}$ (BBR3610, 1,1/*t,t*-6,2,6, **1′**) have been probed using 2D [^{1}H, ^{15}N] HSQC NMR spectroscopy. Reported herein are the rate constants for the hydrolysis of **1** and **1′**, as well as the acid dissociation constants of the coordinated aqua ligands in their aquated derivatives. The aquation and anation rate constants for the single step aquation model in 15 mM $NaClO_4$ (pH 5.4) at 298 K are, for **1**, $k_1 = 7.2 \pm 0.1 \times 10^{-5}$ s^{-1}, $k_{-1} = 0.096 \pm 0.002$ M^{-1} s^{-1} and, for **1′**, $k_1 = 4.0 \pm 0.2 \times 10^{-5}$ s^{-1}, $k_{-1} = 1.4 \pm 0.1$ M^{-1} s^{-1}. The effect of the linker backbone (Pt(tetra(m)mine *vs.* polyamine) was evaluated by comparison with previous data for the trinuclear complex [{*trans*-PtCl(NH$_3$)$_2$}$_2$(μ-*trans*-Pt(NH$_3$)$_2$\{NH$_2$(CH$_2$)^{6}NH$_2$\}$_2$)]$^{4+}$ (1,0,1/*t,t,t*or BBR3464). The pK_1 for 1,0,1/*t,t,t*(3.44) is closest to that of **1** (3.12), while the pronounced difference for **1′** (4.54), means that **1′** is the least aquated of the three complexes at equilibrium. pK_a values of 5.92 were calculated for the aquated forms of both **1** and **1′**, which are 0.3 p*K*units higher than for either 1,0,1/*t,t,t*, or the dinuclear 1,1/*t,t*. The higher pK_a values for both polyamine-linked compounds may be attributed to the formation of macrochelates between the central NH$_2$ groups and the {PtN$_3$O}coordination sphere of the aquated species.

Introduction

Polynuclear platinum complexes (PPCs) belong to a family of novel anticancer therapeutics that are designed based on the hypothesis that structures that are fundamentally different from the mononuclear platinum complex, cisplatin, should exhibit novel DNA binding and antitumour properties.[1] The dinuclear complex, [{*trans*-PtCl(NH$_3$)$_2$}$_2$(μ-NH$_2$(CH$_2$)$_6$NH$_2$)]$^{2+}$ (1,1/*t,t*or BBR3005), and the trinuclear complex, [{*trans*-PtCl(NH$_3$)$_2$}$_2$(μ-*trans*-Pt(NH$_3$)$_2$\{NH$_2$(CH$_2$)$_6$NH$_2$\}$_2$)]$^{4+}$ (1,0,1/*t,t,t*or BBR3464), Scheme 1, are two such examples of this class of anticancer therapeutics, and both exhibit significantly enhanced cytotoxicity compared to cisplatin and its derivatives.[1,2] Whilst cisplatin

†Electronic supplementary information (ESI) available: Scientist equation used to fit the data for the aquation of **1** and **1′** (Model S1), ^{1}H NMR spectra of **1** and **1′** in 15 mM Na perchlorate at pH 5.4 and 298 K (Fig. S1) and ^{15}N {^{1}H} DEPT NMR spectra of **1** and **1′** in 15 mM Na phosphate, pH 5.4, 298 K (Fig. S2).

This journal is © The Royal Society of Chemistry 2011

*s.berners-price@griffith.edu.au; Fax: +61 (0)7 5552 8220; Tel: 61 +(0)7 5552 8033.

NIH-PA Author Manuscript
NIH-PA Author Manuscript
NIH-PA Author Manuscript

NIH-PA Author Manuscript

NIH-PA Author Manuscript

NIH-PA Author Manuscript

predominantly forms short-range intra- and inter-strand crosslinks, 1,1/*t,t* and 1,0,1/*t,t,t*both contain one or more flexible hexanediamine linkers that allow for the formation of long-range intra- and inter-strand {Pt,Pt}DNA crosslinks.[3–6] Another distinguishing feature of both complexes is that they are positively charged (2^+ and 4^+, respectively). This feature has been shown to facilitate binding to DNA, through preassociative electrostatic and H-bonding interactions.[5] Cytotoxicity and cellular accumulation have also been shown to be charge-dependent.[1,7] 1,0,1/*t,t,t*has undergone Phase I[8] and Phase II[9,10] clinical trials, the only $Pt_{(II)}$ agent structurally distinct from cisplatin and its analogs to do so. The products of degradation in blood plasma can be replicated by reactions with sulfur-containing proteins such as glutathione.[11,12]

Due to their biological relevance, namely in cell proliferation, polyamines have been exploited in drug design with several recent reviews highlighting advances in the field.[13,14] We have previously shown that incorporation of a linear polyamine such as spermidine or spermine into the basic framework, and replacement of the central tetraa(m)mine unit of PPCs, produces a series of dinuclear compounds with significant cytotoxic and antitumour activity compared to 1,0,1/*t,t,t*.[15–17] The complexes [{*trans*-$PtCl(NH_3)_2$}$_2${μ-$(NH_2(CH_2)_6NH_2(CH_2)_6NH_2)$}]$^{3+}$ (BBR3007, 1,1/*t,t*-6,6 or **1**) and [{*trans*-$PtCl(NH_3)_2$}$_2${μ-$(NH_2(CH_2)_6NH_2(CH_2)_2NH_2(CH_2)_6NH_2)$}]$^{4+}$ (BBR3610/CTI3610, 1,1/*t,t*-6,2,6 or **1′**) (Scheme 1) are two further examples. Complex **1′** is one of the most potent platinum complexes reported and is of special interest because it and it's derivatives are potential "2nd-generation" PPCs for clinical trials.[18–21] The global DNA binding profile is similar to those of 1,0,1/*t,t,t*.[22] The cytotoxicity of BBR3007 is lower than BBR3610 but this also depends on other factors besides DNA binding such as cellular accumulation.[15]

The substitution-labile chloride ligands of the terminal Pt am(m)ine coordination spheres in PPCs exchange readily for aqua ligands in aqueous medium, with an ensuing equilibrium between the aqua and hydroxo species (see Scheme 2).[1] 2D [^{1}H, ^{15}N] HSQC NMR spectroscopy has been routinely used to study the aquation chemistry of ^{15}N-labelled Pt am(m)ine complexes, and allows for all platinated species to be observed at micromolar concentrations.[23–29] It has been used also to monitor the mechanism and rates of formation of long-range interstrand crosslinks by PPCs in DNA.[3,5,6,30]

Given the clinical relevance of **1′** and its derivatives, we have begun a comparison of its DNA binding profile with the "parent" clinical agent 1,0,1/*t,t,t*.[31] In that study the role of the central NH^2 groups in the spermine-like linker of **1′** was also probed, by comparison with the spermidine-like derivative **1**. Reported in this paper is a study of the solution behavior of both **1** and **1′**, including measurement of the pK_a values of the coordinated water ligands in their aquated derivatives. These values are of interest because the aquated species is more reactive than its hydroxo counterpart in the context of DNA binding.

Results

Fully ^{15}N-labelled **1** and **1′** were prepared by adaptations of published procedures,[15,32] involving synthesis of the polyamine linkers as ^{15}N-derivatives, followed by coupling with two equivalents of monoactivated ^{15}N-transplatin.

2D [^{1}H, ^{15}N] HSQC NMR spectra were recorded over time to examine the spectral changes upon aquation, as previously reported.[26,27] Representative spectra are shown in Fig. 1, the collated ^{1}H and ^{15}N chemical shifts are listed in Table 1 and the aquation profiles are shown in Fig. 2. The pK_a values of the coordinated aqua ligands were calculated from the pH profiles of Fig. 3.

NIH-PA Author Manuscript

NIH-PA Author Manuscript

NIH-PA Author Manuscript

Aquation behavior of 1 and 1′

Aquation studies for both **1** and **1′** were carried out in 15 mM $NaClO_4$ at pH 5.4 and 298 K, allowing direct comparison with previous aquation studies of 1,0,1/*t,t,t*.[26] At this pH, the crosspeaks in the Pt–$^{15}NH_3$ region of the 2D [^{1}H, ^{15}N] HSQC spectra are free from overlap, enabling the spectral changes corresponding to hydrolysis to be monitored over time. Complex **1** took 6 h to reach equilibrium, whilst **1′** achieved equilibrium after 2 h.

Fig. 1a shows a 2D [^{1}H, ^{15}N] HSQC NMR spectrum of **1** after the sample had reached equilibrium. Two major crosspeaks in the Pt–$^{15}NH_3$ region at δ 3.85/– 64.5 and 4.08/–62.2 ppm are assigned to the dichloro species, **1**, and the {PtN_3O}end (**2b**) of the monoaqua monochloro species, **2**, respectively. Corresponding crosspeaks in the Pt–$^{15}NH_2$ region are observed at δ 4.98/–47.0 ppm (**1**) and 5.08/–64.2 ppm (**2b**). This change in the $^{15}NH_2$ chemical shift of Δδ = 17.2 ppm is consistent with the displacement of the *trans* chloro group with an aqua ligand and is similar to that reported previously for 1,0,1/*t,t,t*.[26]

A 2D [^{1}H, ^{15}N] HSQC NMR spectrum of the solution of **1′** after reaching equilibrium is shown in Fig. 1b. The ^{1}H/^{15}N chemicals shifts of the Pt–$^{15}NH_3$ groups are δ 3.85/–64.5 (**1′**) and 4.08/–62.2 ppm (**2b′**) and are identical to those observed for **1**. In the Pt–$^{15}NH_2$ region, the corresponding crosspeaks are at δ 4.98/–47.0 (**1′**) and 5.08/–64.3 ppm (**2b′**). The crosspeaks corresponding to the {PtN^3Cl} moiety of the monoaqua monochloro species, **2a** and **2a′**, in both the Pt–$^{15}NH_3$ and Pt–$^{15}NH_2$ regions, are overlapped with those of the dichloro species (**1** and **1′**).

Table 1 compares the ^{1}H/^{15}N chemical shifts of the Pt–$^{15}NH_3$ and Pt–$^{15}NH_2$ groups of **1**, **1′** and their aquated derivatives, as well as the corresponding species for 1,0,1/*t,t,t*[26] and no significant differences are observed.

The proposed reaction pathway for the aquation of both **1** and **1′** is shown in Scheme 2, along with the model used in the analysis of the kinetic data, which assumes that both complexes undergo a single aquation step. The time dependent changes in concentration of the species detected during the aquation are shown in Fig. 2, along with the curves of best fit to the kinetic model. The rate constants and derived equilibrium constants are listed in Table 2, in comparison to those of 1,0,1/*t,t,t*.[26]

pK_a determination of the aquated derivatives of 1 and 1′

To determine the pK_a values of the coordinated aqua ligands, solutions of **1** and **1′** (in 15 mM Na phosphate), that had reached equilibrium over a 24 h period, were titrated across the pH range ~2–10. The pH dependent changes in the ^{1}H/^{15}N chemical shifts of the Pt–$^{15}NH_3$ groups of the terminal {PtN_3O}moieties of the aquated derivatives **2** and **2′**, were measured by 2D [^{1}H, ^{15}N] HSQC NMR spectroscopy (see Fig. 3). Identical pK_a values of 5.92 ± 0.02 were derived from the change in ^{1}H chemical shifts for the aquated derivatives of both compounds. The pH titration of **1** was also carried out in 100 mM $NaClO_4$ and an identical pK_a value was obtained. Interestingly, this value is 0.3 pK units higher than that of the aquated forms of both 1,1/*t,t* and 1,0,1/*t,t,t*(5.62) (measured in 100 mM $NaClO_4$).[26,27]

Analysis of the central polyamine linker groups of 1 and 1′

The polyamine-linked complexes have the advantage that ^{15}N-labelling of the central NH_2 groups allows interrogation by 2D [^{1}H, ^{15}N] HSQC NMR methods and helps delineate the role of central charge in the overall profile of these agents. The central NH_2 groups, for both **1** and **1′**, were only clearly visible in the [^{1}H,^{15}N] HSQC NMR spectra at lower pH and there are interesting differences between the two compounds apparently related to the presence of the central ethylenediamine unit in **1′**.

NIH-PA Author Manuscript

NIH-PA Author Manuscript

NIH-PA Author Manuscript

A ^{1}H NMR spectrum recorded for **1**, at pH 5.4 in 15 mM $NaClO_4$ (Fig. S1a†) shows clearly four resonances corresponding to the four inequivalent –CH_2– groups (1–6) in the alkyl chain (see Scheme 1). The chemical shifts of these resonances are listed in Table 3. The 1 and 6 –CH_2– groups show ^{15}N-coupling ($^{2}J(^{1}H–^{15}N)$ = 7.79 Hz) as a consequence of their proximity to the terminal Pt–$^{15}NH_2$ and central $^{15}NH_2$ groups, respectively. For **1′**, five ^{1}H NMR resonances are observed (Fig. S1b†) corresponding to the inequivalent –CH_2– protons of the alkyl chain (1–7; see Scheme 1), and the chemical shifts (for 1–6) are similar to those observed for **1** (Table 3). Surprisingly, no ^{15}N splitting is observed for the –$(CH_2)_2$– protons (7) which are bonded to the central $^{15}NH_2$ groups. For the ^{15}N-labelled complex, these –CH_2– protons constitute the AA′ part of an A2XX′A2′ spin system, as a result of unequal ^{15}N–^{1}H spin–spin coupling to the two ^{15}N atoms. A similar spin-system is observed for the bidentate phosphines with –$(CH_2)_2$– backbones, such as $Ph_2P(CH_2)_2PPh_2$ (dppe), where a quasi-triplet is observed for these protons.[33] The ^{15}N {^{1}H}DEPT NMR spectrum of **1**, at pH 5.4, clearly shows a ^{15}N resonance at δ 25.7 ppm assignable to the central –$^{15}NH_2$– group in the polyamine chain (Fig. S2a†), however for **1′**, no ^{15}N resonance correlating to the central –$^{15}NH_2(CH_2)_2{}^{15}NH_2$– was observed under these conditions (Fig. S2b†).

Fig. 4a shows the central $^{15}NH_2$ region of the 2D [^{1}H, ^{15}N] HSQC NMR spectrum of **1** at pH 2.5 (after allowing the sample to reach equilibrium). The major crosspeak (δ 7.88/25.7 ppm) is assigned to the central NH_2 group of the dichloro species, as it correlates with the resonance observed in the ^{1}H spectrum recorded of a freshly prepared sample (Fig. S1a†) and the ^{15}N{^{1}H} DEPT spectrum (Fig. S2a†). The crosspeak at δ 7.10/30.2 ppm is assigned to the central NH_2 groups of the monoaqua monochloro species, **2**, and the crosspeak at δ 7.46/12.0 ppm to the terminal NH_3^+ group of a dangling primary amine, most likely arising from acidic cleavage of the Pt–NH_2R bond. As the pH is increased the crosspeaks diminish in intensity. At pH 4.5 the peak for **2** was no longer visible but that for **1** was still present, albeit weaker in intensity. The crosspeaks for **1** and the dangling amine species (*d*) were no longer visible above pH 5.7 and pH 5.2, respectively.

Fig. 4b shows the 2D [^{1}H, ^{15}N] HSQC NMR spectrum and the corresponding ^{1}H NMR spectrum of the central $^{15}NH_2$ group of **1′** at pH 2.1. The ^{1}H/^{15}N crosspeak at δ 7.98/25.6 ppm is assigned to the dichloro species and is deshielded in the ^{1}H dimension by δ 0.1 ppm compared to the analogous crosspeak for **1** (see above). The ^{1}H/^{15}N crosspeak at δ 7.10/31.1 ppm is assigned to the central NH_2 groups of the monoaqua monochloro species, **2′**. The most intense ^{1}H/^{15}N crosspeak observed at δ 7.50/12.0 ppm correlates with a doublet of triplets centered at δ 7.49 ppm in the ^{1}H NMR spectrum (splitting = 72 Hz) and is assigned, as for **1**, to a Pt by-product with a dangling amine and shows the characteristic splitting pattern.[12] Further evidence for the assignment is a small resonance at δ 3.01 ppm in the ^{1}H NMR spectrum (labelled ′*d*′, Fig. S1b†) assigned to the CH_2 group nearest the terminal NH_3^+ moiety. In the [^{1}H,^{15}N] HSQC NMR spectrum the ^{1}H/^{15}N crosspeak corresponding to the central $^{15}NH_2$ group of the aquated species, **2′**, was no longer visible above pH 3.5 whilst the analogous crosspeaks for the dichloro species **1′** and the dangling amine impurity (d) disappeared as the pH was raised to pH 4.1 and pH 4.9, respectively.

Discussion

2D [^{1}H, ^{15}N] HSQC NMR spectroscopy is a powerful tool in the understanding of the aquation profile of ^{15}N-labelled platinum am(m)ine anticancer complexes. The aquation and acid dissociation constants of two fully ^{15}N-labelled novel platinum anticancer complexes, **1**

†Electronic supplementary information (ESI) available: Scientist equation used to fit the data for the aquation of **1** and **1′** (Model S1), ^{1}H NMR spectra of **1** and **1′** in 15 mM Na perchlorate at pH 5.4 and 298 K (Fig. S1) and ^{15}N {^{1}H} DEPT NMR spectra of **1** and **1′** in 15 mM Na phosphate, pH 5.4, 298 K (Fig. S2).

NIH-PA Author Manuscript

NIH-PA Author Manuscript

NIH-PA Author Manuscript

and **1′**, have been studied under conditions similar to those previously used for 1,0,1/*t,t,t*, allowing for a direct comparison.[26]

There is literature precedence for the ^{15}N chemical shifts of ^{15}N-labelled free polyamines (such as putriscene, spermine and spermidine)[34] but no Pt-based anticancer complexes with ^{15}N-labelled polyamine linkers have been investigated previously. An interesting aspect of the ^{15}N-{^{1}H} and [^{1}H,^{15}N] HSQC NMR spectra of the platinated polyamines is that the observation of resonances for the central NH_2 groups is pH-dependent. For **1**, the ^{1}H/^{15}N resonance for the central $^{15}NH_2$ group in the polyamine chain is visible below pH 5.7. The ^{15}N chemical shift (δ 25 ppm) is in agreement with previous studies on related ^{15}N-labelled free polyamines.[34–36] However for **1′**, the ^{1}H/^{15}N resonance for the central $–^{15}NH_2(CH_2)_2{}^{15}NH_2–$ moiety is not observed above pH 4.1. Perrin showed that decreasing the number of $–CH_2–$ groups between the two terminal amine groups of diamines (such as $H_2N(CH_2)_2NH_2$, $H_2N(CH_2)_3NH_2$, $H_2N(CH_2)_4NH_2$), increased the difference between the two acid dissociation constants pK_{a1} and pK_{a2}.[37] For ethylenediamine pK_{a1} is 9.9–10.2 and pK_{a2} is 6.8–7.5. It is not expected that the pK_a of the central linker will change dramatically upon platination.[38] Discrete ^{15}N chemical shifts for various polyamines (spermine, spermidine, thermospermine and thermine)[34,35] have been observed over the pH range 5.9–12.5. In all cases, however, the $–^{15}NH_2–$ groups are separated by at least three $–CH_2–$ groups. The absence of the corresponding resonances for the ethylenediamine moiety of **1′** under the experimental conditions may be attributed to the close proximity of the two $–NH_2–$ groups. At pH > 4.1 ^{1}H exchange between the two ^{15}N atoms may broaden the signals out beyond detection. This phenomenon is not observed in the case of **1** as there is only one central amine group; the central NH_2 resonance is clearly observed.

The aquation studies of **1** and **1′** reveal interesting differences compared to 1,0,1/*t,t,t*. For the forward reaction ($Pt–Cl \rightarrow Pt–OH_2$), the rate constants for both polyamine-linked complexes are lower than that of 1,0,1/*t,t,t*, but more significant for **1′** (2.7-fold lower) than **1** (1.5-fold lower). Similarly, the rate constant for the anation reaction ($Pt–OH_2 \rightarrow Pt–Cl$) is significantly higher for **1′** (1.4 M^{-1} s^{-1}) compared to both **1** (0.096 M^{-1} s^{-1}) and 1,0,1/*t,t,t*(0.294 M^{-1} s^{-1}). Thus, the dichloro species of **1′** is more favoured at equilibrium in comparison to either **1** or 1,0,1/*t,t,t*. Based on these results it is clear that the central NH_2 groups have an influence over the kinetics of the aquation of the terminal {PtN_3Cl} group, whereas it might have been expected that the central linker (be it platinum or amine) is far enough away from the terminal {$PtNH_3Cl$} groups so as not to influence them.

A further point of interest is that the pK_a values of aquated derivatives of both **1** and **1′** (5.92) are 0.3 p*K*units higher than that of 1,0,1/*t,t,t* or 1,1/*t,t*. Hence at physiological pH for both complexes there will be a greater proportion of the more reactive aquated species (and less of the less reactive hydroxo species) compared to 1,0,1/*t,t,t*. A possible explanation for this difference is the formation of a hydrogen bond between the central NH_2 group and the aqua ligand of the terminal {PtN_3O} moiety (see Fig. 5). The flexibility of the linker will help in this regard. Formation of such a macrochelate could explain also the large ^{1}H chemical shift changes of the central NH_2 groups upon aquation (Fig. 4). Notably, the ^{1}H/^{15}N shifts of the aquated species of both **1** and **1′** in phosphate and perchlorate buffers are similar (Fig. 4) and the pK_a value of the aquated derivatives are also the same in the different electrolytes. In studies of the interaction of the related 1,1/*c,c* with PO_4^{3}, a macrochelate species with phosphate bridging between the two Pt groups was characterized.[27] The distance between the two terminal Pt groups in 1,1/*c,c*is identical to the distance between the terminal Pt groups and the central NH_2 groups of **1** and **1′**. Further, a unique glutathione-bridged moiety producing a novel 11-membered chelate ring was also observed with 1,1/*c,c*.[39] The nature of the macrochelate is however different in the present case. Formation of the phosphate-bridged macrochelate is facilitated by the *cis* geometry of

NIH-PA Author Manuscript

NIH-PA Author Manuscript

NIH-PA Author Manuscript

the Pt–NH_3 groups in 1,1/*c,c*. Both **1** and **1′**, have *trans*Pt–NH_3 groups and hence the electrolyte does not play a role in the macrochelate formation.

Conclusion

The two novel dinuclear polyamine-linked platinum antitumour complexes **1** and **1′** exhibit interesting aquation chemistry compared to 1,0,1/*t,t,t*and 1,1/*t,t*. Clear evidence for the effect on aquation of the central amine motifs has been found, suggesting novel solution behavior which merits further investigation. BBR3610 was designed to have the same distance between the Pt–Cl units as BBR3464, with the central ethylenediamine unit mimicking the Pt(tetraamine) unit of BBR3464 with respect to hydrogen-bonding and electrostatic interactions.[16] The observation of macrochelate species in the present case suggests that there is significantly more conformational flexibility with the polyamine linker – or in essence the central Pt(tetraamine) unit in BBR3464 induces some conformational rigidity in the trinuclear species, which may be reflected in its' reactions with biomolecules. The polyamine linkers influence both the kinetics of the aquation reactions and the pK_a values of the coordinated water ligands, compared to the trinuclear (central Pt(tetra(m)mine linker) case. The global DNA binding profile of BBR3610 is similar to that of BBR3464.[22] Kinetic studies of substitution of BBR3610 by small molecules such as methionine and 5′-GMP,[20] also suggest a broadly similar profile in aqueous medium to that of BBR3464, with likelihood of similar degradation (metabolism) profiles for polyamine-bridged species in comparison to that of the trinuclear drug.[12,20] The use of less substitution-labile leaving groups[21] or use of different geometries (1,1/*c,c*) by use of 1,2-dach carrier groups[22,40] are valid approaches to systematically alter the pharmacokinetic profile of the PPCs.

Experimental

Synthesis of compounds

[{*trans*-PtCl($^{15}NH_3$)$_2$}$_2${μ-($^{15}NH_2$(CH$_2$)$_6$$^{15}NH_2$(CH$_2$)$_6$$^{15}NH_2$)}]$^{3+}$(1) and [{*trans*-PtCl($^{15}NH_3$)$_2$}$_2${μ-($^{15}NH_2$(CH$_2$)$_6$$^{15}NH_2$(CH$_2$)$_2$-$^{15}NH_2$(CH$_2$)$_6$$^{15}NH_2$)}]$^{4+}$ (1′). The fully ^{15}N-labelled derivatives of **1** and **1′** were prepared by adaptations of published procedures.[15,32] The general strategy is to synthesize the fully ^{15}N-labelled linkers with the central $^{15}NH_2$ amine groups blocked using the *tert*-butyloxycarbonyl (BOC) protecting group. The protected linker is then incorporated into the dinuclear compound by reaction with two equivalents of monoactivated transplatin (*trans*-[$PtCl_2$($^{15}NH_3$)$_2$]) – deprotection and removal of the central BOC protecting groups affords the desired fully ^{15}N-labelled **1** and **1′**.

NMR spectroscopy

The NMR spectra were recorded using a Bruker 600 MHz spectrometer (^{1}H, 599.92 MHz; ^{15}N, 60.79 MHz). The ^{1}H shifts were referenced internally to TSP (sodium-3-trimethylsilyl-D_4-propionate) and the ^{15}N shifts were referenced externally to $^{15}NH_4Cl$ (1.0 M in 1.0 M HCl in 5% D_2O/95% H_2O) (δ = 0.0 ppm). 2D [^{1}H, ^{15}N] HSQC NMR spectra were recorded using the pulse sequence of Stonehouse *et al.*[41] 1D ^{15}N {^{1}H} DEPT NMR spectra were recorded using a *zgig* pulse sequence with WALTZ decoupling[42] optimized for ^1J(^{15}N–^{1}H) = 72 Hz and a 90° pulse of 12.75 μs, with 256 transients recorded over a period of 1.5 h. Continuous wave (CW) decoupling in the ^{1}H NMR spectra was achieved by irradiating the desired resonances at a power level of 15 dB at the frequency of the Pt–$^{15}NH_3$ group in the 1D ^{15}N {^{1}H} DEPT NMR spectra.

NIH-PA Author Manuscript

NIH-PA Author Manuscript

NIH-PA Author Manuscript

pH measurements

The pH values were measured using a Shindengen ISFET (semiconductor) pH meter (pH Boy-KS723 (SU-26F) and calibrated against buffers of pH 4.0, 6.9 and 10.0. To avoid leaching of chloride ions, 5 μL samples were placed on the electrode and the pH recorded without returning the aliquot to the sample. Adjustments to the pH were carried out using 0.02, 0.05, 0.1 or 0.5 M solutions of either $HClO_4$ or NaOH in 5% D_2O/95% H_2O.

Aquation studies

Solutions were prepared by dissolving **1** (0.80 mg, 0.85 μmol) or **1′** (0.35mg, 0.33 μmol) in $NaClO_4$ (478 μL, 15 mM) in 5%D_2O/95% H_2O with TSP (2 μL, 13.3 mM) to give initial concentrations of 1.80 mM and 0.69 mM of **1** and **1′**, respectively. A series of ^1H and 2D [^1H, ^{15}N] HSQC NMR spectra were recorded at 298 K, until equilibrium conditions were attained. For the 1D {^1H} ^{15}N DEPT experiments, solutions of **1** (2.00 mg, 2.13 μmol) or **1′** (0.70 mg, 0.67 μmol) in Na phosphate (478 μL, 15 mM) were prepared in 5% D_2O/95% H_2O with TSP (2 μL, 13.3 mM), to give initial concentrations of 4.44 mM and 1.39 mM of **1** and **1′**, respectively.

Data analysis

Concentrations of species were determined by measuring peak volumes in the Pt–$^{15}NH_3$ region of the 2D [^1H, ^{15}N] HSQC NMR spectra using the plug-in "2D NMR Analysis" developed for the program ImageJ.[43] Peak volumes were converted into concentrations relative to the initial concentration of the dichloro species of **1** or **1′**. The concentrations of **1** and **2** (and **1′** and **2′**) at each time point were derived based on the relative volumes of the Pt–$^{15}NH_3$ crosspeaks after correcting for peak overlap, according to the single aquation model, as described previously.[26] Differential equations were used to fit to either first- or second-order rate equations. The aquation rate constants were determined using a non-linear optimization process using SCIENTIST (Version 2.0, MicroMath Inc.) with errors reported for one standard deviation.

pK_a determination of the aquated derivatives of 1 and 1′

Solutions of **1** and **1′** (in 15 mM Na phosphate), that had reached equilibrium over a 24 h period, were titrated across the pH range ~2–10. Adjustments in pH were performed using 0.02, 0.05, 0.1 or 0.5 M solutions of either $HClO_4$ or NaOH in 5% D_2O/95% H_2O. For each pH point, 1D ^1H and 2D[^1H, ^{15}N] HSQC NMR spectra were recorded and changes in the ^1H and ^{15}N chemical shifts of the Pt–$^{15}NH_3$ groups of the {PtN_3O} moiety (**2b** and **2b′**) were monitored.

Kaleidagraph (Synergy Software, Reading, PA) was used to analyze the pH titration data using eqn (1):

$$\delta=(\delta_A[H^+]+\delta_B K_a)/([H^+]+K_a) \quad (1)$$

where K_a is the acid dissociation constant for the Pt–OH_2 group of the aquated species and δ_A and δ_B are the chemical shifts of the aqua and the hydroxo species, respectively. Fig. 3 shows the pH titration curves that have been fit to eqn (1) for the aquated derivatives of both **1** and **1′**.

Supplementary Material

Refer to Web version on PubMed Central for supplementary material.

NIH-PA Author Manuscript

NIH-PA Author Manuscript

NIH-PA Author Manuscript

Acknowledgments

The authors thank the University of Western Australia for a University Postgraduate Award (RAR). This work was supported by the Australian Research Council (Discovery Grants to SBP and NF (DP0662817 and DP1095383) and the National Institutes for Health (ROI-CA78754). We thank Dr Lindsay Byrne for assistance in acquiring the NMR spectra.

References

1. Farrell N. Met. Ions Biol. Syst. 2004; 42:251–296. [PubMed: 15206105]
2. Perego P, Caserini C, Gatti L, Carenini N, Romanelli S, Supino R, Colangelo D, Viano I, Leone R, Spinelli S, Pezzoni G, Manzotti C, Farrell N, Zunino F. Mol. Pharmacol. 1999; 55:528–534. [PubMed: 10051537]
3. Cox JW, Berners-Price SJ, Davies MS, Qu Y, Farrell N. J. Am. Chem. Soc. 2001; 123:1316–1326. [PubMed: 11456703]
4. Kasparkova J, Zehnulova J, Farrell N, Brabec V. J. Biol. Chem. 2002; 277:48076–48086. [PubMed: 12226099]
5. Hegmans A, Berners-Price SJ, Davies MS, Thomas DS, Humphreys AS, Farrell N. J. Am. Chem. Soc. 2004; 126:2166–2180. [PubMed: 14971952]
6. Ruhayel RA, Moniodis JJ, Yang X, Kasparkova J, Brabec V, Berners-Price SJ, Farrell NP. Chem.–Eur. J. 2009; 15:9365–9374. [PubMed: 19691069]
7. Montero EI, Benedetti BT, Mangrum JB, Oehlsen MJ, Qu Y, Farrell NP. Dalton Trans. 2007:4938–4942. [PubMed: 17992278]
8. Sessa C, Capri G, Gianni L, Peccatori F, Grasselli G, Bauer J, Zucchetti M, Vigano L, Gatti A, Minoia C, Liati P, Van S, den Bosch, Bernareggi A, Camboni G, Marsoni S. Ann. Oncol. 2000; 11:977–983. [PubMed: 11038034]
9. Jodrell DI, Evans TRJ, Steward W, Cameron D, Prendiville J, Aschele C, Noberasco C, Lind M, Carmichael J, Dobbs N, Camboni G, Gatti B, De Braud F. Eur. J. Cancer. 2004; 40:1872–1877. [PubMed: 15288289]
10. Hensing TA, Hanna NH, Gillenwater HH, Camboni MG, Allievi C, Socinski MA. Anti-Cancer Drugs. 2006; 17:697–704. [PubMed: 16917215]
11. Vacchina V, Torti L, Allievi C, Lobinski R. J. Anal. At. Spectrom. 2003; 18:884–890.
12. Oehlsen ME, Qu Y, Farrell N. Inorg. Chem. 2003; 42:5498–5506. [PubMed: 12950196]
13. Casero RAJ, Woster PM. J. Med. Chem. 2009; 52:4551–4573. [PubMed: 19534534]
14. Senanayake MDT, Amunugama H, Boncher TD, Casero RA, Woster PM. Essays Biochem. 2009; 46:77–94. [PubMed: 20095971]
15. Rauter H, Di Domenico R, Menta E, Oliva A, Qu Y, Farrell N. Inorg. Chem. 1997; 36:3919–3927.
16. Farrell, NP.; Spinelli, S. Uses of Inorganic Chemistry in Medicine. Farrell, NP., editor. Royal Society of Chemistry; 1999. p. 124-134.
17. McGregor TD, Hegmans A, Kasparkova J, Neplechova K, Novakova O, Penazova H, Vrana O, Brabec V, Farrell N. JBIC, Biol. Inorg. Chem. 2002; 7:397–404.
18. Billecke C, Finniss S, Tahash L, Miller C, Mikkelsen T, Farrell NP, Bogler O. Neuro-Oncology. 2006; 8:215–226. [PubMed: 16723633]
19. Mitchell C, Kabolizadeh P, Ryan J, Roberts JD, Yacoub A, Curiel DT, Fisher PB, Hagan MP, Farrell NP, Grant S, Dent P. Mol. Pharmacol. 2007; 72:704–714. [PubMed: 17578896]
20. Summa S, Maigut J, Puchta R, van Eldik R. Inorg. Chem. 2007; 46:2094–2104. [PubMed: 17311374]
21. Gatti L, Perego P, Leone R, Apostoli P, Carenini N, Corna E, Allievi C, Bastrup U, De Munari S, Di Giovine S, Nicoli P, Grugni M, Natangelo M, Pardi G, Pezzoni G, Singer JW, Zunino F. Mol. Pharmaceutics. 2010; 7:207–216.
22. Zerzankova L, Suchankova T, Vrana O, Farrell NP, Brabec V, Kasparkova J. Biochem. Pharmacol. 2010; 79:112–121. [PubMed: 19682435]
23. Berners-Price SJ, Frenkiel TA, Frey U, Ranford JD, Sadler PJ. J. Chem. Soc., Chem. Commun. 1992:789–791.

NIH-PA Author Manuscript

NIH-PA Author Manuscript

NIH-PA Author Manuscript

24. Berners-Price SJ, Ronconi L, Sadler PJ. Prog. Nucl. Magn. Reson. Spectrosc. 2006; 49:65–98.
25. Davies MS, Cox JW, Berners-Price SJ, Barklage W, Qu Y, Farrell N. Inorg. Chem. 2000; 39:1710–1715. [PubMed: 12526558]
26. Davies MS, Thomas DS, Hegmans A, Berners-Price SJ, Farrell N. Inorg. Chem. 2002; 41:1101–1109. [PubMed: 11874344]
27. Zhang J, Thomas DS, Davies MS, Berners-Price SJ, Farrell N. JBIC, Biol. Inorg. Chem. 2005; 10:652–666.
28. Cubo L, Quiroga AG, Zhang J, Thomas DS, Carnero A, Navarro-Ranninger C, Berners-Price SJ. Dalton Trans. 2009:3457–3466. [PubMed: 19381408]
29. Cubo L, Thomas DS, Zhang J, Quiroga AG, Navarro-Ranninger C, Berners-Price SJ. Inorg. Chim. Acta. 2009; 362:1022–1026.
30. Zhang J, Thomas DS, Berners-Price SJ, Farrell N. Chem.–Eur. J. 2008; 14:6391–6405. [PubMed: 18537208]
31. Ruhayel RA, Oke M-J, Langner J, Farrell N, Berners-Price SJ. manuscript in preparation.
32. Farrell, N.; Menta, E.; DiDomenico, R.; Spinelli, S. US Pat. 6 022 892. 2000.
33. Harris RK. Can. J. Chem. 1964; 42:2275–2281.
34. Frydman L, Rossomando PC, Frydman V, Fernandez CO, Frydman B, Samejima K. Proc. Natl. Acad. Sci. U. S. A. 1992; 89:9186–9190. [PubMed: 1409623]
35. Takeda Y, Samejima K, Nagano K, Watanabe M, Sugeta H, Kyogoku Y. Eur. J. Biochem. 1983; 130:383–389. [PubMed: 6297905]
36. Fernández CO, Buldain G, Samejima K. Biochim. Biophys. Acta, Protein Struct. Mol. Enzymol. 2000; 1476:324–330.
37. Perrin, DD. Acid Dissociation Constants of Organic Bases in Aqueous Solution. London: Butterworths; 1965.
38. Hegmans A, Kasparkova J, Vrana O, Kelland LR, Brabec V, Farrell NP. J. Med. Chem. 2008; 51:2254–2260. [PubMed: 18338842]
39. Oehlsen ME, Hegmans A, Qu Y, Farrell N. Inorg. Chem. 2005; 44:3004–3006. [PubMed: 15847402]
40. Williams JW, Qu Y, Bulluss GH, Alvorado E, Farrell NP. Inorg. Chem. 2007; 46:5820–5822. [PubMed: 17592835]
41. Stonehouse J, Shaw GL, Keller J, Laue ED. J. Magn. Reson., Ser. A. 1994; 107:178–184.
42. McCoy MA, Mueller L. J. Magn. Reson., Ser. A. 1993; 101:122–130.
43. Ruhayel RA, Corry B, Braun C, Thomas DS, Farrell NP, Berners-Price SJ. Inorg. Chem. 2010; 49:10815–10819. [PubMed: 21067174]
44. Farrell N, Qu Y. Inorg. Chem. 1989; 28:3416–3420.
45. Humphrey W, Dalke A, Schulten K. J. Mol. Graphics. 1996; 14:33–38.

NIH-PA Author Manuscript
NIH-PA Author Manuscript
NIH-PA Author Manuscript

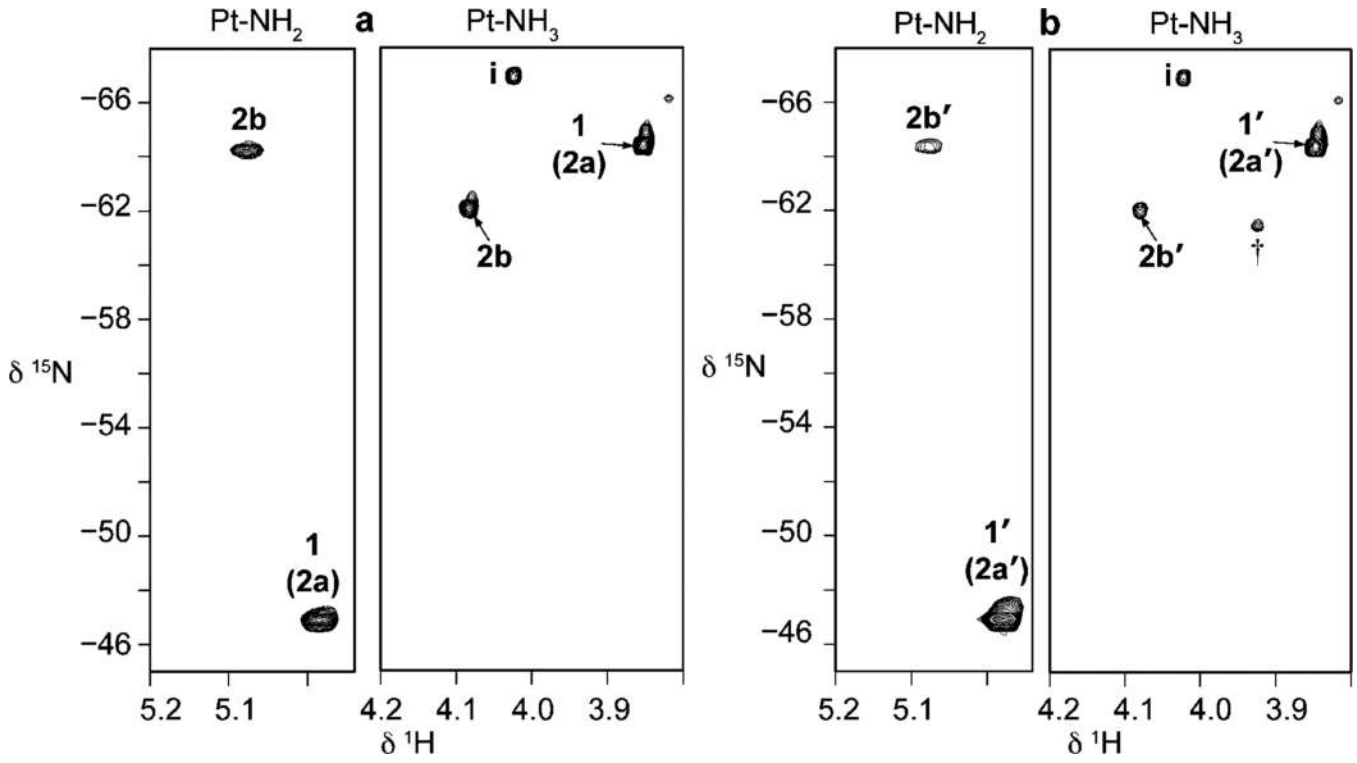

Fig. 1.

2D [^{1}H,^{15}N] HSQC NMR spectra of the Pt–$^{15}NH_3$ and Pt–$^{15}NH_2$ regions of **1** (a) and **1′** (b) in 15 mM $NaClO_4$ (pH 5.4) after reaching equilibrium at 298 K. The crosspeaks are assigned to the dichloro species, **1/1′** and the {PtN_3Cl}(**2a/2a′**) and {PtN_3O}(**2b/2b′**) moieties of the monoaqua monochloro species, **2/2′**, respectively (Scheme 1). In both cases the peak at δ 4.02/– 67.0 ppm (labelled 'i') is assumed to be a ^{15}N tetraam(m)ine Pt impurity and is similar to that observed previously for ^{15}N-1,1/*t,t*.[25] For **1′** the peak at δ 3.93/– 61.3 (labelled †) may be attributed to a polymeric ^{15}N-labelled impurity with dangling amines induced by bis-substitution at the Pt centre, with similar structures previously observed.[44]

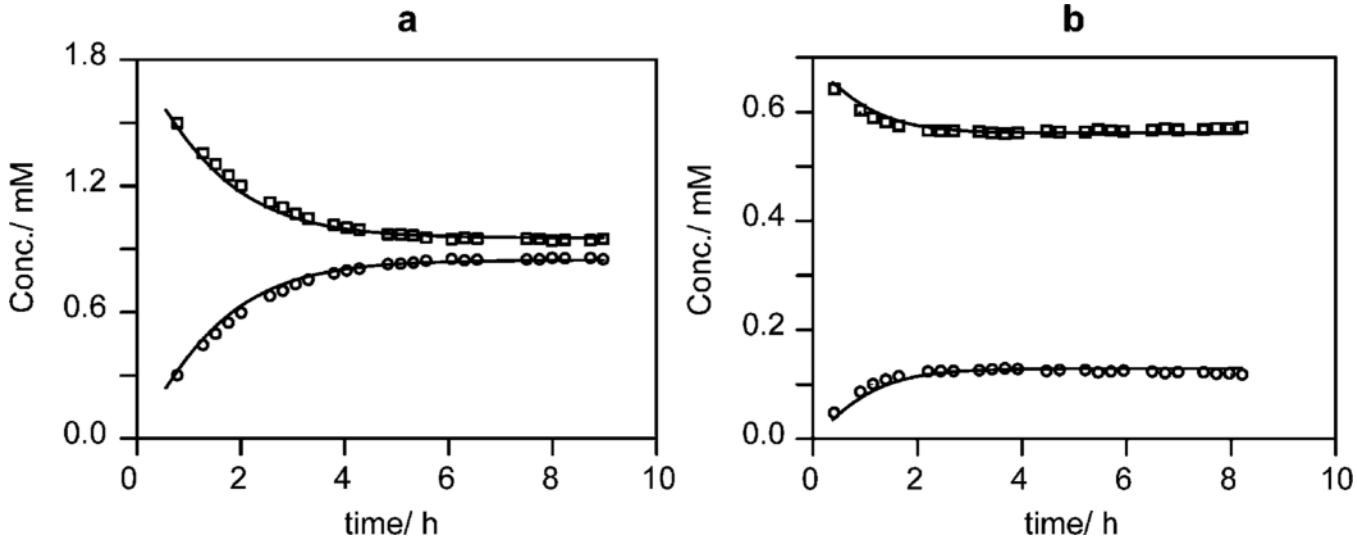

Fig. 2.

Plot of the time dependence of species in the aquation of **1** (a) and **1′** (b) in 15 mM $NaClO_4$ (5% D_2O/95% H_2O) at pH 5.4 and 298 K according to the single aquation model shown in Scheme 2. Key: open squares, the dichloro species **1/1′**, open circles, the monoaqua monochloro species, **2/2′**.

NIH-PA Author Manuscript
NIH-PA Author Manuscript
NIH-PA Author Manuscript

NIH-PA Author Manuscript

NIH-PA Author Manuscript

NIH-PA Author Manuscript

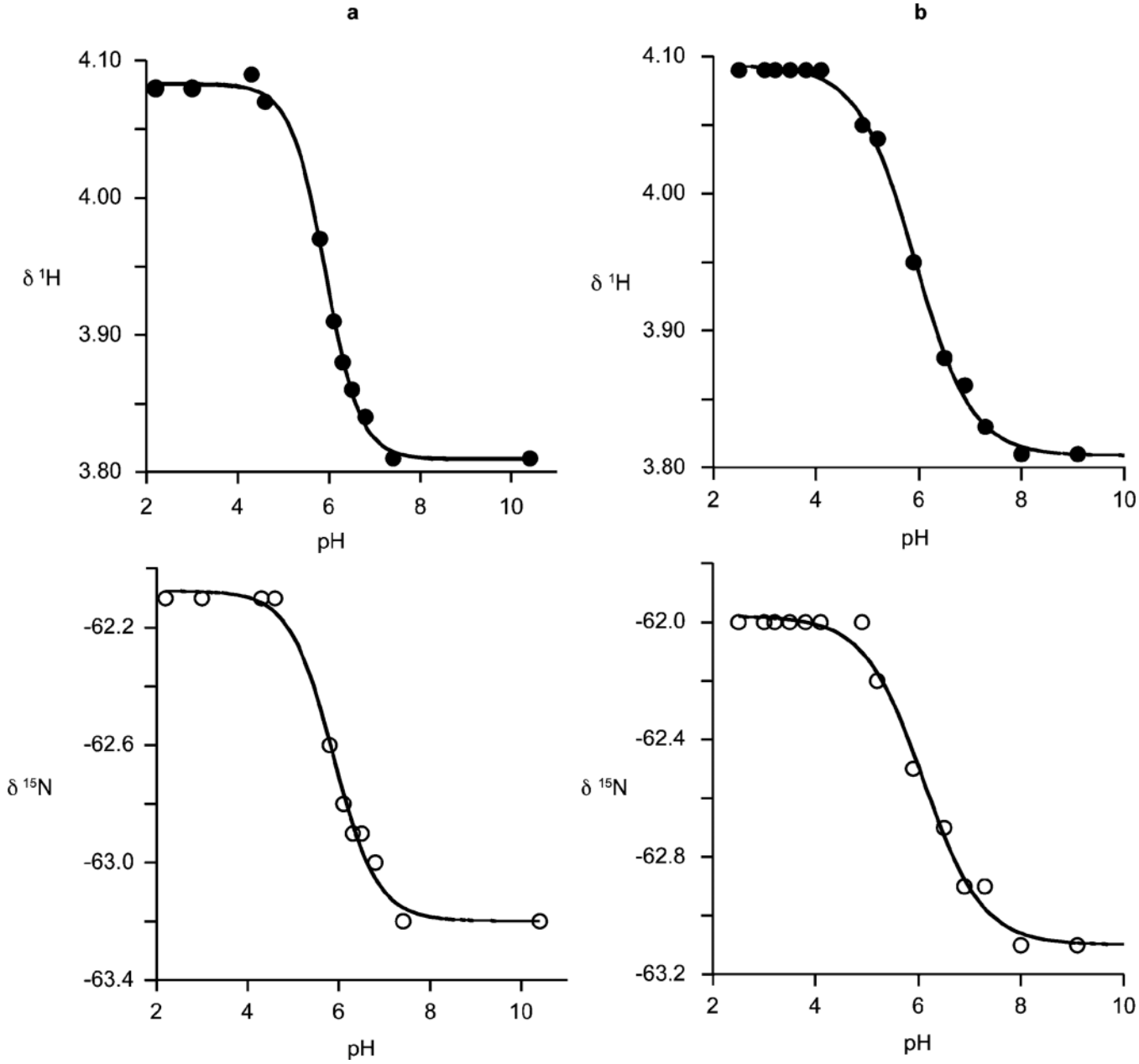

Fig. 3.

Plots of ^{1}H and ^{15}N chemical shifts *vs.* pH for the Pt–$^{15}NH_3$ groups of the monoaquated derivatives of **1** (a) and **1′** (b) in 15 mM Na phosphate.

NIH-PA Author Manuscript
NIH-PA Author Manuscript
NIH-PA Author Manuscript

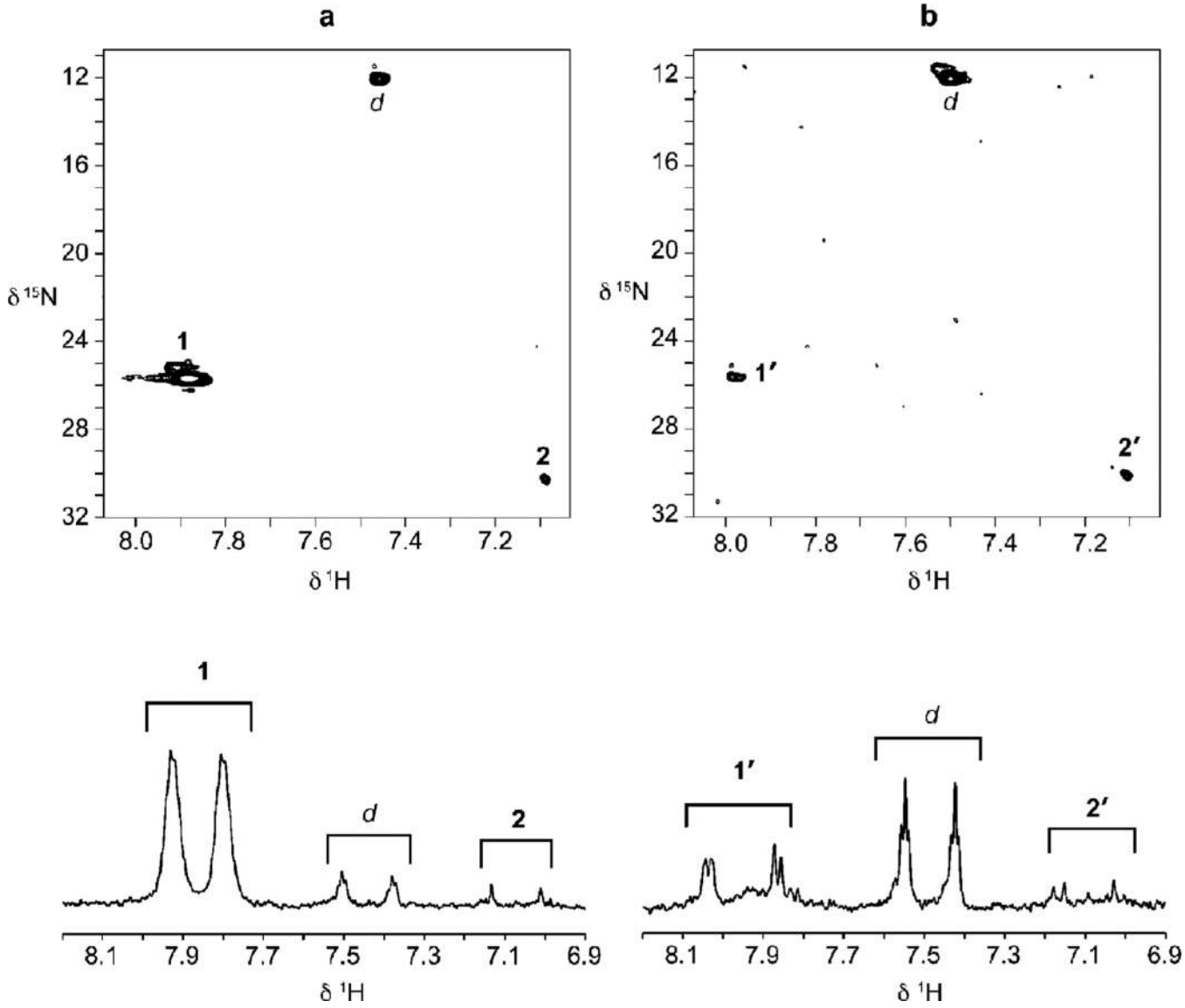

Fig. 4.

The central $^{15}NH_2$ region of the 2D [^{1}H, ^{15}N] HSQC (top) and ^{1}H NMR spectra (bottom) of **1** (pH 2.5 in 100mM $NaClO_4$) (**a**) and **1′** (pH 2.1 in 15 mM Na phosphate) (**b**) showing the dichloro species, **1/1′**, and the aquated derivatives, **2/2′**. Crosspeaks/multiplets labelled '*d*' are assigned to Pt species with a dangling amine, most likely arising from acidic cleavage of the Pt-NH_2R bond (see text). The high relative intensity of these peaks may be explained by a slower exchange with bulk water for NH protons of the terminal 1° amine compared to those of the 2° amine in the linker of **1/1′**.

NIH-PA Author Manuscript

NIH-PA Author Manuscript

NIH-PA Author Manuscript

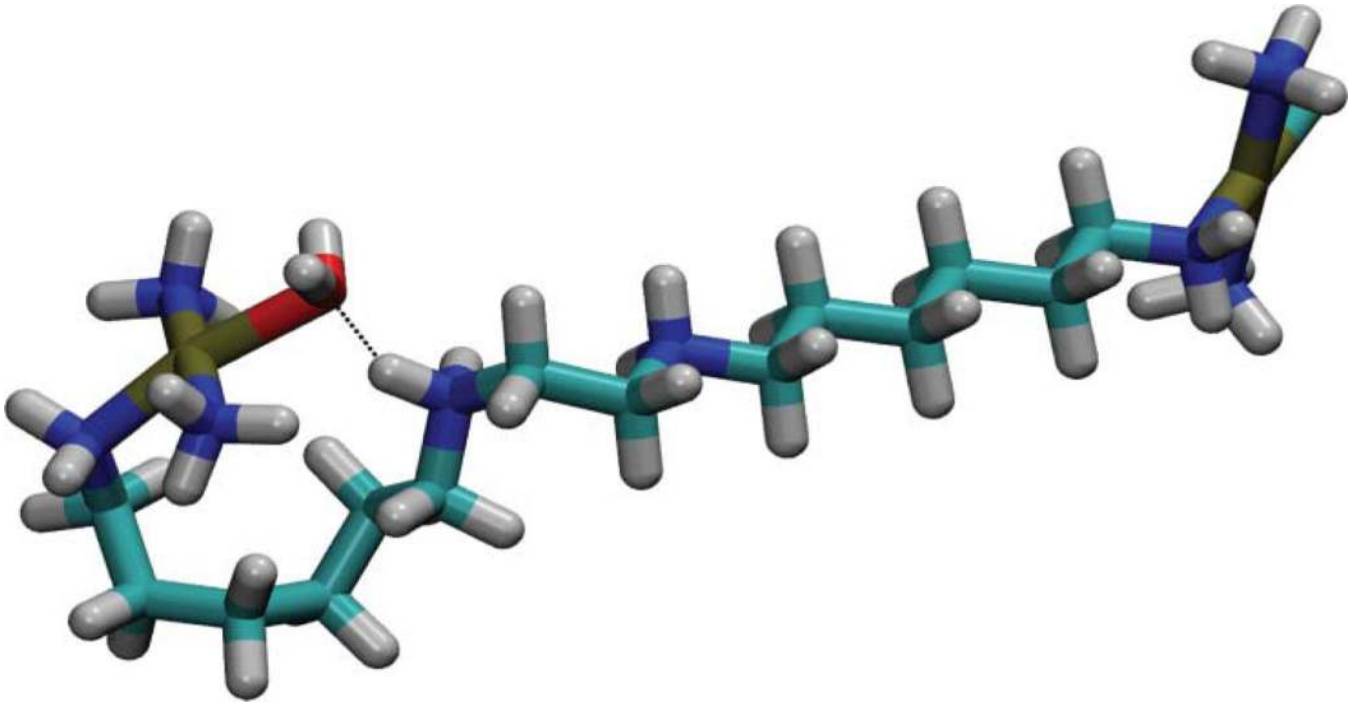

Fig. 5.

Proposed macrochelate structure with a possible H-bond between the terminal $\{PtN_3O\}$ moiety and the central NH_2 groups of the polyamine linker (**1′** has been used as the example). The structure was created using the program package Spartan '08 v1.0.0 (Wavefunction, Inc., Irvine, California). The illustration was created using the program package VMD.[45]

NIH-PA Author Manuscript

NIH-PA Author Manuscript

NIH-PA Author Manuscript

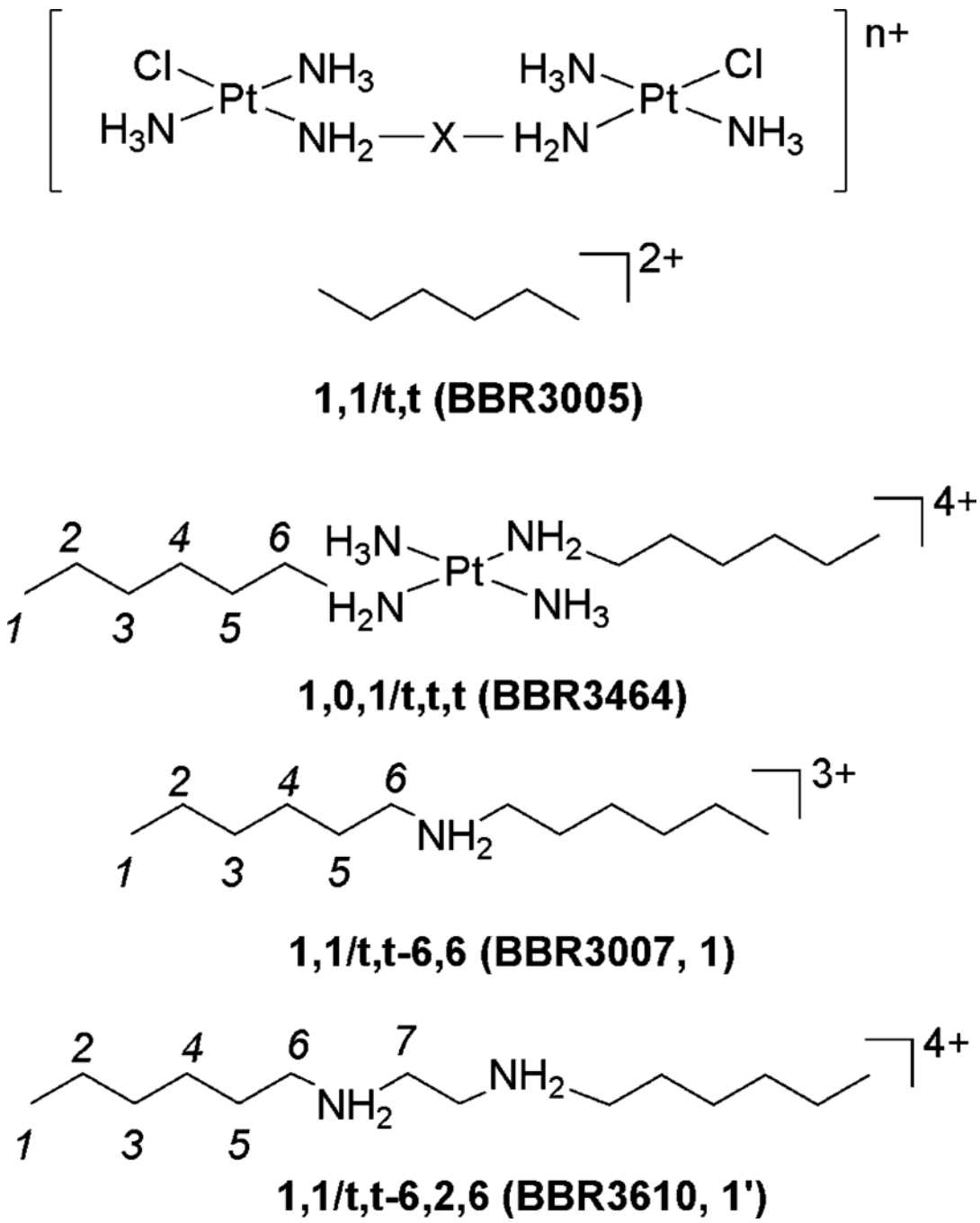

Scheme 1.

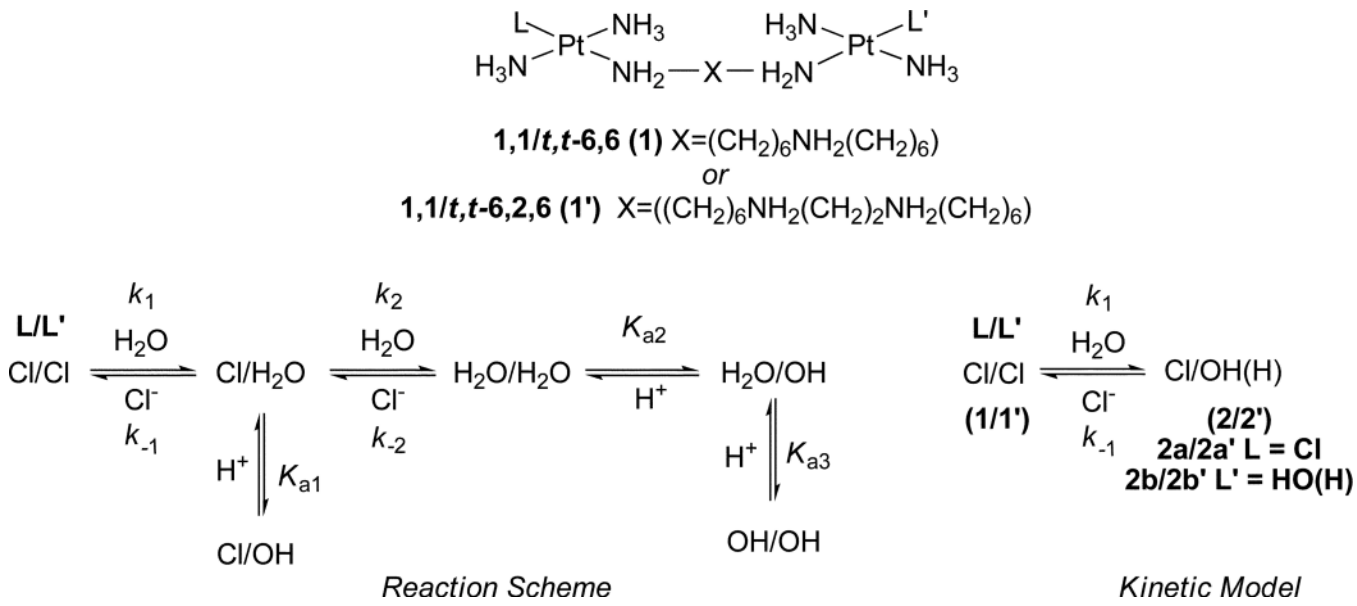

Scheme 2.

NIH-PA Author Manuscript
NIH-PA Author Manuscript
NIH-PA Author Manuscript

NIH-PA Author Manuscript
NIH-PA Author Manuscript
NIH-PA Author Manuscript

Table 1

^{1}H and ^{15}N chemical shifts for the Pt–$^{15}NH_3$ and Pt–$^{15}NH_2$ groups of 1 and 1′ and their aquated derivatives[a]

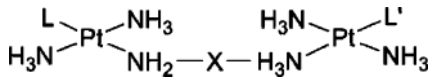

	1,1/*t*,*t*-6,6 (1) [b, d]		**1,1/*t*,*t*-6,2,6 (1′)** [b,e]		**1,0,1/*t*,*t*,*t*** [c]	
Species	Pt–NH_3	Pt–NH_2	Pt–NH_3	Pt–NH_2	Pt–NH_3	Pt–NH_2
L/L′	$\delta^{1}H/^{15}N$	$\delta^{1}H/^{15}N$	$\delta^{1}H/^{15}N$	$\delta^{1}H/^{15}N$	$\delta^{1}H/^{15}N$	$\delta^{1}H/^{15}N$
Cl/Cl	3.85/– 64.5	4.98/– 47.0	3.85/– 64.5	4.98/– 47.0	3.84/– 64.7	4.97/– 46.9
H_2O(OH)/**Cl**	3.85/– 64.5	4.98/– 47.0	3.85/– 64.5	4.98/– 47.0	3.84/– 64.7	4.97/– 46.9
H_2O/Cl[f]	4.08/– 62.1	5.15/– 65.3	4.09/– 62.0	5.16/– 65.3	4.09/– 61.9	5.12/– 65.1
OH/Cl[f]	3.81/– 63.1	4.48/– 56.9	3.81/– 63.1	4.47/– 56.9	3.83/– 63.0	4.46/– 56.9

[a] ^{1}H referenced internally to TSP and ^{15}N referenced externally to $^{15}NH_4Cl$; δ in the ^{15}N dimension is ± 0.2 ppm.

[b] This work.

[c] From ref. 26

[d] At low pH $^{1}H/^{15}N$ crosspeaks for the central $^{15}NH_2$ group of **1** and the aquated species **2** are visible at δ 7.88/–25.7 ppm and δ 7.10/30.2 ppm, respectively (see Fig. 4a).

[e] At low pH $^{1}H/^{15}N$ crosspeaks for the central $^{15}NH_2$ group of **1′** and the aquated species **2′** are visible at δ 7.98/25.6 ppm and δ 7.10/31.1 ppm, respectively (see Fig. 4b).

[f] Values derived from the pH titration curves (Fig. 3).

Dalton Trans. Author manuscript; available in PMC 2012 May 01.

NIH-PA Author Manuscript

NIH-PA Author Manuscript

NIH-PA Author Manuscript

Table 2

Rate and equilibrium constants for the aquation of **1** and **1′** at 298 K in 15 mM $NaClO_4$ (pH 5.4) in comparison to 1,0,1/*t,t,t*[a]

Parameter	1	1′	1,0,1/*t,t,t*[b]
k_1 (10^{-5} s^{-1})	7.2 ± 0.2	4.0 ± 0.2	10.7 ± 0.1
k_{-1} (M^{-1} s^{-1})	0.096 ± 0.002	1.4 ± 0.1	0.294 ± 0.004
pK_1	3.12 ± 0.02	4.54 ± 0.06	3.44 ± 0.04

[a]Values derived using the single aquation model shown in Scheme 2.

[b]From ref. 26

NIH-PA Author Manuscript

NIH-PA Author Manuscript

NIH-PA Author Manuscript

Table 3

^{1}H chemical shifts of the alkyl CH_2 groups of **1** and **1′**[a]

–CH_2–	**1**	**1′**	**1,0,1/*t*,*t*,*t*[b]**
1[c]	2.69	2.68	2.68
2	1.68	1.70	1.68
3	1.39	1.39	1.38
4	1.39	1.39	1.38
5	1.69	1.70	1.68
6[c]	3.03	3.11	2.68
7	—	3.42	—

[a] For numbering scheme see Scheme 1; ^{1}H chemical shifts referenced to TSP.

[b] From ref. 26

[c] $^2J(^1H–^{15}N)$ = 7.79 Hz.